

Biogeosciences Discussions is the access reviewed discussion forum of *Biogeosciences*

Temporal variability of the anthropogenic CO₂ storage in the Irminger Sea

F. F. Pérez¹, M. Vázquez-Rodríguez¹, E. Louarn², X. A. Padín¹, H. Mercier³, and A. F. Ríos¹

¹Instituto de Investigaciones Marinas, CSIC, Eduardo Cabello 6, 36208 Vigo, Spain

²Laboratoire de Chimie Marine, Institut Universitaire Européen de la Mer et UMR CNRS UPMC 7144 Roscoff, Plouzané, France

³Laboratoire de Physique des Océans, CNRS Ifremer IRD UBO, IFREMER Centre de Brest, B.P. 70 29280 Plouzané, France

Received: 29 February 2008 – Accepted: 10 March 2008 – Published: 11 April 2008

Correspondence to: F. F. Pérez (fiz.perez@iim.csic.es)

Published by Copernicus Publications on behalf of the European Geosciences Union.

1587

Abstract

The anthropogenic CO₂ (C_{ant}) estimates from cruises spanning more than two decades (1981–2006) in the Irminger Sea area reveal a large variability of the C_{ant} storage rates in the North Atlantic Subpolar Gyre. During the early 1990's, the C_{ant} uptake rates doubled the average rate for 1981–2006, whilst a remarkable drop to almost half that average followed from 1997 onwards. The C_{ant} storage evolution runs parallel to CFC12 inventories and is in good agreement with C_{ant} uptake rates of increase calculated from sea surface pCO₂ measurements. The North Atlantic Oscillation shift from a positive to a negative phase in 1996 led to a reduction of the air-sea heat loss in the Labrador Sea. The consequent convection weakening accompanied by an increase in stratification lowered the efficiency of the northern North Atlantic CO₂ sink.

1 Introduction

The ocean is a CO₂ sink that during the 1990s has removed 2.2±0.4 Pg C·yr⁻¹ from the atmosphere out of the total 8.0±0.5 Pg yr⁻¹ of anthropogenic carbon (C_{ant}) emitted to the atmosphere directly from human activities (Canadell et al., 2007). The North Atlantic Subpolar Gyre (NASPG) has the largest C_{ant} storage per unit area (~80 mol C·m⁻² on average) of all oceans, holding 38% of the oceanic C_{ant} storage (Sabine et al., 2004). The key mechanism responsible for this large CO₂ uptake is the Meridional Overturning Circulation (MOC). The MOC transports warm surface waters with high C_{ant} loads from low latitudes to the northern North Atlantic (Watson et al., 1995; Wallace et al., 2001), where the deep convection and entrainment by the overflows contribute to store this C_{ant}-laden water at depth. Eventually, these waters will return south with the lower limb of the MOC. Recent studies on the variability of the MOC point towards a possible decrease in its intensity during the second half of the twentieth century (Bryden et al., 2005) and warn about a possible future “shut-down” in response to global warming (McManus et al., 2004). This would bring forth pro-

1588

found consequences for global climate due to the associated decrease in oceanic C_{ant} uptake (Sarmiento and Le Quéré, 1996) and heat transport (Drijfhout et al., 2006). Several Ocean General Circulation Models (OGCMs) have suggested that the decadal variability of the MOC is closely related with the variability of Labrador Seawater (LSW) formation rates (Böning et al., 2006). On the other hand, the long-term evolution of the MOC such as the possible weakening during the 21st century might be related to a decrease in the density of the Denmark Strait Overflow Water (DSOW) and the Iceland-Scotland Overflow Water (ISOW) (Böning et al., 2006). These water masses meet in the Irminger Sea, where the Deep Western Boundary Current originates (Yashayaev et al., 2008).

The Irminger basin has been proposed as a LSW formation region (Pickart et al., 2003), in addition to the Labrador Sea. Independently of the formation region, two modes of LSW are typically defined: the classical LSW (cLSW, sometimes referred to as deep LSW) and the less dense upper LSW (uLSW) (Kieke et al., 2006). The LSW is formed in winter, when deep convection caused by intense air-sea heat loss results in the formation of homogeneous layers of up to 2000 m. The ambient stratification and wind forcing intensity are determinant factors in this convective process (Dickson et al., 1996; Curry et al., 1998; Lazier et al., 2002). During the early 1990's, the strongly positive North Atlantic Oscillation (NAO) index forced an impressive convection activity down to more than 2000 m (Lazier et al., 2002). This resulted in the formation of the thickest layer of cLSW observed in the past 60 years (Curry et al., 1998). This energetic convection period abruptly ended in 1996 with the shift of the NAO index to a negative phase. Nonetheless, weaker convection events continued to take place in the central Labrador Sea and formed the less dense uLSW. It was first detected in the western side of the Labrador Sea during the second half of the 1990's (Azetsu-Scott et al., 2003; Stramma et al., 2004). Decadal time series of layer thicknesses of both LSW types corroborate that, far from exceptional, uLSW is an important product of the convection activity in the Labrador Sea (Kieke et al., 2007). These time series show that the strong formation processes of cLSW in the early 1990's are actually the exceptional

1589

events. The temporal evolution of CFCs in the Labrador Sea indicates that after a strong increase in the early 1990's, CFC12 concentrations started to decline towards the end of the decade in the cLSW body (Azetsu-Scott et al., 2003). This CFC12 decrease was also observed during the early 2000's in the Labrador and Irminger Seas (Kieke et al., 2007). The fluctuations of convection in the NASPG can modify the expected oceanic C_{ant} uptake rates in a likewise and parallel manner to CFCs.

In this study we have gathered hydrographical measurements and results from seven cruises conducted in the Irminger Sea. The aim is twofold: *a*) study the evolution of C_{ant} concentrations in subsurface waters, LSW, North East Atlantic Deep Water (NEADW) and DSOW in order to *b*) evaluate the variability of the oceanic uptake rates of C_{ant} linked to the fluctuations of the convective processes in the NASPG, and the reduction of the formation of cLSW.

2 Dataset and method

Six cruises spanning through 25 years (1981–2006) of high-quality carbon measurements in the Irminger Sea area have been selected for this study (Fig. 1, Table 1). Unlike in the most recent cruises from FOUREX or the OVIDE project, the TTO-NAS analytics did not include certified reference materials for their total inorganic carbon (C_T) measurements. For the TTO-NAS, Tanhua et al. (2005) performed a cross-over analysis with an overlapping more recent cruise. Based on a comparison with modern Certified Reference Material-referenced data, they suggest a correction for TTO-NAS C_T measurements of approximately $-3.0 \mu\text{mol}\cdot\text{kg}^{-1}$, which has been applied to our dataset. In order to evaluate and interpret the variations of C_{ant} uptake rates we have focused on six water masses delimited by the density (σ_θ) intervals established following Kieke et al. (2007) and Yashayaev et al. (2008), namely: from the upper 100 m to $\sigma_\theta=27.68 \text{ kg}\cdot\text{m}^{-3}$ we find the subsurface layer; The uLSW is found between $27.68 < \sigma_\theta < 27.76 \text{ kg}\cdot\text{m}^{-3}$; cLSW between $27.76 < \sigma_\theta < 27.81 \text{ kg}\cdot\text{m}^{-3}$; North East Atlantic Deep Water (NEADW, which includes the ISOW contributions) is delimited by

1590

$27.81 < \sigma_{\theta} < 27.88 \text{ kg}\cdot\text{m}^{-3}$, and DSOW by $\sigma_{\theta} > 27.88 \text{ kg}\cdot\text{m}^{-3}$ (Fig. 1b).

To estimate the anthropogenic CO_2 the φC_T^o method from Vázquez-Rodríguez et al. (2008)¹ is applied. It is a data-based, back-calculation method that constitutes an improved version of the classical ΔC^* approach (Gruber et al., 1996). The φC_T^o method uses 100–200 m data as the only reference to build the parameterizations needed. This sub-surface layer avoids the seasonal variability of surface properties, thus making the derived parameterizations more representative of water mass formation conditions. The method does not rely on CFC measurements and takes into account the temporal variation of the CO_2 air-sea disequilibrium (ΔC_{dis}). The overall uncertainty of the method has been estimated in $5.2 \mu\text{mol}\cdot\text{kg}^{-1}$ by means of random error propagation over the precision limits of the parameters involved in the calculation of C_{ant} . Regarding the specific inventory estimates, errors were estimated using a perturbation procedure for each layer and the total water column. They were calculated by means of random propagation with depth of a $5.2 \mu\text{mol}\cdot\text{kg}^{-1}$ standard error of the C_{ant} estimate over 100 perturbation iterations, and are plotted on Fig. 3.

3 Results

The salinity, potential temperature (θ), apparent oxygen utilisation ($\text{AOU} = \text{O}_2^{\text{eq}} - \text{O}_2^{\text{meas}}$, which represents the sum of the biological activity undergone by the sample since it was last in equilibrium with the atmosphere) and C_{ant} in the Irminger Basin from 1981 to 2006 are shown in Fig. 2. The TTO-NAS shows a strong vertical stratification at the LSW level between the first 1000 m and the relative salinity maximum of the NEADW (>34.95), related to the low convection activity in the Labrador Sea in the late 1970's (Kieke et al., 2006). It must be reminded that it takes two years for the LSW to spread

¹Vázquez-Rodríguez, M., Padin, X. A., Pérez, F. F., Ríos, A. F., and Bellerby, R. G. J.: Anthropogenic carbon determination from sub-surface boundary conditions, *Deep-Sea Res. I*, in review, 2008.

1591

into the Irminger Sea (Yashayaev et al., 2008). The temperature minimum ($\theta < 1.5^\circ\text{C}$) in the DSOW is also remarkable within the considered time-span. Compared to TTO-NAS, the AR7E (1991) cruise shows cooler LSW. The strong vertical homogenisation down to 1800 m in 1991 suggests local LSW formation at the Irminger Sea, which caused the saltier NEADW signal to shrivel. The same year, the LSW layer also thickened substantially in the Labrador Sea (Kieke et al., 2006). In 1997, the low salinity LSW invaded lower layers, beyond the 2000 m depth, while surface stratification slightly increased. The temperature of the cLSW reaches its minimum values for the period of observation, in agreement with Yashayaev et al. (2008). The DSOW temperature signature ($\theta < 2^\circ\text{C}$) practically disappeared during the FOUREX cruise, but recovered during the OVIDE cruises history, most importantly in 2004. It is likely that this variability is linked to that of the entrainment downhill of the sills. Alternatively, it must be noted that the FOUREX cruise intersects the DWBC to the south of the OVIDE line, and this may partially account for this difference. During this period of biennial sampling (2002, 2004 and 2006) an increase in salinity (especially at the LSW and NEADW layers) and stratification is observed, coinciding with a period of weak winter convection (Kieke et al., 2006). The described thermohaline evolution concurs with the θ/S results shown by Yashayaev et al. (2008) for the LSW core: A salinity and temperature minimum is recorded in 1996 at the Irminger Sea (which is two years behind the θ/S minimum at the Labrador Sea) followed by a progressive salinization and warming due to lateral mixing that can be observed along the $\sigma_1 = 36.93$ isopycnal and extends to the rest of LSW density range.

In 1981, the AOU profiles nicely separate close to air-sea equilibration subsurface waters from the old NEADW. The relative AOU minimum at the bottom West of the Irminger Basin indicates the marked presence of DSOW. The C_{ant} concentrations follow a similar pattern to AOU: high values, close to saturation ($32 \mu\text{mol}\cdot\text{kg}^{-1}$), near the surface and lower values ($\sim 45\%$ of saturation) towards the bottom. During the first deep convection events in the early 1990's there is a significant and parallel increase in the C_{ant} and oxygen loads in the upper 1500 m. Nevertheless, the NEADW region

1592

shows higher AOU along with slightly lower (around 15%) C_{ant} values than in 1981, denoting the presence of older waters. The high ventilation of the water column caused by the strong deep convection between 1991 and 1997 (Kieke et al., 2006) resulted in smaller AOU and higher C_{ant} values during FOUREX than previously recorded for the LSW in the Irminger Basin. In 1997, the C_{ant} concentrations ($30 \pm 0.7 \mu\text{mol}\cdot\text{kg}^{-1} \approx 80\%$ saturated) at the LSW core is at a maximum and AOU at a minimum. The NEADW layer is richer in oxygen, less saline and it contains about 50% more C_{ant} than in 1991, suggesting that more intense mixing processes occurred with the upper bounding LSW layer. In the CGFZ, where LSW and NEADW flow in opposite direction, mixing processes are enhanced, and in 1997 the LSW transport in this area was particularly intense (Lherminier et al., 2007). During the OVIDE period, convection was weak in the Labrador Sea (Kieke et al., 2006) and no deep convection was recorded in the Irminger Sea (Yashayaev et al., 2008) resulting in a re-stratification of the water column and an aging of the deep-water masses. This is particularly evident in the cLSW, whose AOU increased by $10 \mu\text{mol}\cdot\text{kg}^{-1}$ on average from 2002 to 2006. Also, subsurface (Fig. 1b) C_{ant} levels keep rising in response to the atmospheric CO_2 increase. Conversely, weaker winds and buoyancy forcing associated to the low NAO index period during OVIDE provoked an increase in the stratification of the upper layers. This precluded local ventilation and translated into a dilution of C_{ant} in the cLSW layer due to the permanently active isopycnal mixing. The C_{ant} in the NEADW increases continuously suggesting incorporation of young water by entrainment downhill of the Iceland-Scotland sills. Finally, the DSOW flow (Olsson, 2001) appears more ventilated with respect to previous years and it also displays small C_{ant} relative maxima.

The average values and associated errors of salinity, temperature, AOU, C_{ant} and saturation concentration of $C_{\text{ant}}(C_{\text{ant}}^{\text{sat}})$ for each cruise and layer (Fig. 1) are summarised on Table 2. The average thickness of the layers and their percentage contribution to C_{ant} specific inventories are also given in Table 2. The thickness was calculated as the average distance between layers weighed by the separation between stations. The averages for the rest of properties were computed integrating vertically and horizon-

1593

tally, and then dividing by the area of the corresponding layer. The $C_{\text{ant}}^{\text{sat}}$ is estimated from the average temperature and salinity of the layer, assuming full equilibrium of surface waters with the average atmospheric molar fraction of CO_2 ($x\text{CO}_2$) at the year of each cruise. A quantitative evaluation of the previously described interdependences between the variability of AOU, C_{ant} and ventilation has been attempted by plotting the percentage of $C_{\text{ant}}^{\text{sat}}$ vs. AOU from Table 2. The term $\%C_{\text{ant}}^{\text{sat}}$ is independent of the atmospheric CO_2 increase since it is referred to the $C_{\text{ant}}^{\text{sat}}$ concentration in the corresponding sampling year. In this sense, $\%C_{\text{ant}}^{\text{sat}}$ is comparable to oxygen, whose atmospheric concentration is stationary. Hence, it is expected that recently equilibrated (young) waters will have low AOU and high $\%C_{\text{ant}}^{\text{sat}}$ values, while the opposite is expected in older waters that have undergone large remineralization of organic matter. We found that the largest temporal variability of AOU and $\%C_{\text{ant}}^{\text{sat}}$ is in the cLSW layer, where both variables are highly correlated ($R^2=0.94$). The uLSW shows also a significant $\%C_{\text{ant}}^{\text{sat}}$ vs. AOU correlation ($R^2=0.74$). When all Irminger Sea water masses in Table 2 (except for the DSOW) are considered altogether a correlation of $R^2=0.91$ is obtained. This suggests that in the Irminger Sea, $\%C_{\text{ant}}^{\text{sat}}$ for the sampling year could be estimated fairly accurately from AOU in the main water masses. Hence, for a given AOU value the $\%C_{\text{ant}}^{\text{sat}}$ would be invariable, independently from the sampling year. Knowing the $\%C_{\text{ant}}^{\text{sat}}$ and the atmospheric $p\text{CO}_2$ for the sampling year, C_{ant} could thereby be estimated. This AOU vs $\%C_{\text{ant}}^{\text{sat}}$ dependence establishes an empirical quantitative relationship based on a simplified mixing model with subsurface waters and NEADW as end-members. The former would represent the highly ventilated young waters from the winter mixed layer (WML) whereas the latter would stand for the older components. The deviations from this hypothetical mixing line can be due to lateral advection, to interannual or decadal variability of water mass formation or to differential biological activity rates.

The temporal evolution of the average C_{ant} in each of the five layers is plotted in Fig. 3. The subsurface layer (Fig. 1b) increases its C_{ant} steadily and sustains its high $\%C_{\text{ant}}^{\text{sat}}$ (>86%) while trying to catch up with the rising atmospheric CO_2 concentra-

1594

tions. The uLSW trend from 1981 to 1991 follows its upper bound subsurface layer, keeping up with the atmospheric CO₂ increase and maintaining its %C_{ant}^{sat}. The maximum thinning of the uLSW layer from 1981 to 1997 coincides with the end of the maximum convection period in the Irminger Sea (Kieke et al., 2006). The cLSW almost doubled its thickness and average C_{ant} content during this period of time at a rate even superior to the atmospheric one. All of it derives from the increased convection processes that occurred in the NASPG between 1991 and 1997 (Kieke et al., 2006). The noteworthy decrease in C_{ant} and layer thickness during the OVIDE cruises caused by the hindered ventilation entails the increase in the AOU levels due to isopycnal mixing. In the NEADW layer, C_{ant} shows a large increment from 1991 to 1997 parallel to the salinity and AOU drop. This suggests the possibility of important diapycnal mixing with the upper re-ventilated cLSW. The DSOW layer will represent a very small proportion in terms of total storage in the Irminger basin given its short thickness. It shows an analogous behaviour to NEADW, i.e., there is an increase in average C_{ant} from 1991 to 1997, matched with a drop in AOU caused by the incorporation of young water by entrainment downhill of the Iceland-Scotland sills. Regarding the total storage, its temporal evolution shows a global increase at different paces. From 1981 to 2006 the average rate of increase in the specific C_{ant} storage for the Irminger Sea has been $1.1 \pm 0.1 \text{ mol C} \cdot \text{m}^{-2} \cdot \text{yr}^{-1}$. During the early 1990's, this rate was more than twice the mean ($2.3 \pm 0.6 \text{ mol C} \cdot \text{m}^{-2} \cdot \text{yr}^{-1}$). Compared with this period of exacerbated C_{ant} storage rate in the Irminger Sea, the average C_{ant} uptake during the following decade (1997–2006) underwent an important fall (Fig. 3) that was estimated in $-1.5 \pm 0.4 \text{ mol C} \cdot \text{m}^{-2} \cdot \text{yr}^{-1}$. The average C_{ant} storage rate of $0.75 \pm 0.16 \text{ mol C} \cdot \text{m}^{-2} \cdot \text{yr}^{-1}$ during the FOUREX-OVIDE period was found to be significantly different from that of the early 1990's (p-value > 0.05).

1595

4 Discussion

As Doney and Jenkins (1988) pointed out, ocean regions affected by strong convection processes tend to acquire large air-sea disequilibria. This applies not only to CO₂, but also to atmospheric gases with higher air-sea transfer velocities such as oxygen or CFCs. The same processes affecting oceanic C_{ant} uptake will be determining the distribution and uptake rates of CFCs. Several works have focused on the CFCs in the NASPG after the 1970's, and the patterns they described support the C_{ant} trends obtained in the present study. The specific inventories of CFC12 in the core of the cLSW found in both the Labrador and Irminger Seas grew until approximately the first half of the 1990's. As Lazier et al. (2002) have illustrated, the formation of cLSW ceased after 1997. The lack of supply of low-salinity/CFC-rich surface waters led to an annual increase in cLSW salinities and a decrease in CFCs because of isopycnal mixing. The CFC12 inventories started to decline strongly from 1997 to 1999 and kept decreasing at a slower rate until 2003 (Azetsu-Scott et al., 2003; Kieke et al., 2007). These evidences seem to correspond with the same pattern here observed for the average C_{ant} in the cLSW, which decreases from 1997 to 2002 (Fig. 3). According to Azetsu-Scott et al. (2003), the marked increase in CFC12 concentrations in the Irminger basin prior to 1995 in the uLSW core reduced to almost standstill from that point until 2001. This result is also in good agreement with the patterns of average C_{ant} obtained for the same years and region in this study (Fig. 3). Kieke et al. (2007) have pointed that this significant increase in CFC12 inventories in the uLSW for the NASPG best describes the situation in the Labrador Sea, rather than in the Irminger, where the CFC12 inventory has a more subtle increase during that period. In spite of this remark, our C_{ant} results for the uLSW in the Irminger follow the expected trend, within the associated error margins. With respect to the NEADW and DSOW, Azetsu-Scott et al. (2003) have shown that from 1991 to 2000 the CFC12 storage in the Irminger Sea increased up to 80% in both the NEADW and DSOW layers. Whilst this happened at a steady rate in the case of NEADW, the interannual variability was larger for DSOW.

1596

Over the same period, the C_{ant} storages here obtained increased by 50% and 40% in the NEADW and DSOW layers, respectively. There are a few differences in the environmental behavior of CFCs and CO_2 that may account for the dissimilarities in magnitude of their inventories. The former is not affected by the Revelle factor, it has a greater solubility in cold waters and its atmospheric rate of increase is different to that of CO_2

Although the NASPG has a net gain of C_{ant} by horizontal advection (Mikaloff-Fletcher et al., 2006; Álvarez et al., 2003), estimating how much it is stored and how much of that comes from direct exchange with the atmosphere entails certain difficulty. Indirect estimates of the air-sea C_{ant} fluxes can be obtained by combining C_{ant} storage results with horizontal transports into carbon budget balances from closed box studies (as in Mikaloff-Fletcher et al., 2006). The C_{ant} storage rate for the Irminger Sea was first estimated by Álvarez et al. (2003) in $1.5 \pm 0.3 \text{ mol C} \cdot \text{m}^{-2} \cdot \text{yr}^{-1}$. This number was obtained from the mean penetration depth (MPD) equation as of Broecker et al. (1979) using data from the WOCE A20 and FOUREX cruises for the 1990–1997 time period. The MPD is defined as the quotient between the C_{ant} water column inventory and the C_{ant} concentration in the mixed layer ($C_{\text{ant}}^{\text{ml}}$), and it can be interpreted as an index of the convection activity in the considered region. For the calculation, they assumed a fixed C_{ant} rate of increase of $0.85 \mu\text{mol} \cdot \text{kg}^{-1} \cdot \text{yr}^{-1}$ and calculated an average and constant MPD for the Irminger basin of $1739 \pm 381 \text{ m}$ by approximating $C_{\text{ant}}^{\text{ml}} \approx C_{\text{ant}}^{\text{sat}}$ in the corresponding years. The average C_{ant} storage rate for the 1981–2006 period in the Irminger Sea here obtained is $1.1 \pm 0.1 \text{ mol C} \cdot \text{m}^{-2} \cdot \text{yr}^{-1}$. The calculated average MPD for the considered years is $1715 \pm 63 \text{ m}$ (Fig. 3). This is quite in agreement with Álvarez et al. (2003), although the MPD values are seen to vary, especially in the strong convection periods such as from 1991–1997. The $1.5 \pm 0.3 \text{ mol C} \cdot \text{m}^{-2} \cdot \text{yr}^{-1}$ estimate from Álvarez et al. (2003) is larger than the average $1.1 \pm 0.1 \text{ mol C} \cdot \text{m}^{-2} \cdot \text{yr}^{-1}$ here obtained and, anyhow, lower than the estimated rate between 1991–1997 of $2.3 \pm 0.6 \text{ mol C} \cdot \text{m}^{-2} \cdot \text{yr}^{-1}$. Some factors accounting for the temporal variability of C_{ant} storage rates may explain some of these discrepancies, primarily: a) The time variability of the MPD can affect

1597

notoriously the C_{ant} storage rates, especially between 1991 and 1997 (8% larger than the average). There can exist exceptional interannual stages where the storage rates can amount up to twice (1991–1997) or almost half (1997–2006) the long-term average; b) The C_{ant} rate of increase must consider the dependence of the $C_{\text{ant}}^{\text{sat}}$ with temperature, which is intimately connected with the Revelle factor (it describes how the pCO_2 in seawater changes for a given change in C_T , and vice versa). The capacity for ocean waters to take up C_{ant} is inversely proportional to the Revelle factor, which depends on temperature. The C_{ant} rates of storage can change $\sim 2\%$ per $^\circ\text{C}$.

Our observations can also be compared with other works on the secular variation of sea surface pCO_2 . In the NASPG, Lefèvre et al. (2004) reported a mean increase of $1.8 \mu\text{atm} \cdot \text{yr}^{-1}$ between 1982 and 1998. This corresponds to a $\Delta C_T = 0.77 \mu\text{mol} \cdot \text{kg}^{-1}$ per annum for an average sea surface temperature of 5°C in the Irminger Sea. If an average MPD of 1715 m is considered for this region and time period, the above ΔpCO_2 translates into a C_{ant} storage increase rate of $1.35 \text{ mol C} \cdot \text{m}^{-2} \cdot \text{yr}^{-1}$. This is very close to the $1.22 \pm 0.03 \text{ mol C} \cdot \text{m}^{-2} \cdot \text{yr}^{-1}$ estimated here from Fig. 3 for the 1981–1997 period. From sea surface pCO_2 measurements Schuster et al. (2007) showed that the sink of atmospheric CO_2 in the North Atlantic was subject to important interannual variability. They estimated an annual decrease of the North Atlantic uptake of $-1.1 \text{ mol C} \cdot \text{m}^{-2} \cdot \text{yr}^{-1}$ between 1997 and the mid-2000's. They argued that the main causes for this change were the declining rates of wintertime mixing and ventilation between surface and subsurface waters due to increasing stratification. In the present work we have estimated this same rate of decrease to be $-1.6 \pm 0.4 \text{ mol C} \cdot \text{m}^{-2} \cdot \text{yr}^{-1}$ for the 1997–2006 decade in the Irminger Sea. Corbière et al. (2007) estimated an annual increase in wintertime sea surface pCO_2 of $3.0 \mu\text{atm} \cdot \text{yr}^{-1}$ between 1993 and 2003 utilizing data from a shipping route from Iceland to Newfoundland. They attributed this finding principally to the increasing sea surface temperatures linked with the shift of the NAO index into a negative phase after wintertime 1995. According to Schuster et al. (2007), this corresponds to an annual decrease of the C_{ant} storage of $-1.6 \text{ mol C} \cdot \text{m}^{-2} \cdot \text{yr}^{-1}$, which is in excellent agreement with our estimates.

1598

In summary, the general decline of the NASPG CO₂ sink is supported by the data here obtained and it is corroborated by other results like those from Schuster et al. (2007) or Corbière et al. (2007). There is a documented variability of the Labrador Sea deep convection that reached its maximum activity during the early to mid 1990s, correlated with positive NAO phases. The maximum C_{ant} storage rate occurred during this maximum convection period. The observed convection decrease since 1997 in the NASPG is mainly tied to the enhanced stratification and the consequent reduced heat loss in the northern North Atlantic (Lazier et al., 2002; Azetsu-Scott et al., 2003; Kieke et al., 2007). All these fluctuations are embodied in the NAO index variability. The above factors have a direct influence on the physical pump of CO₂ and add to the changes in the buffer capacity of surface waters to aggravate the capacity of the North Atlantic as a CO₂ sink.

Acknowledgements. This work was developed and funded by the OVIDE research project from the French oceanographic research institution IFREMER and by the European Commission within the 6th Framework Programme (EU FP6 CARBOOCEAN Integrated Project, Contract no. 511176). M. Vázquez-Rodríguez is funded by Consejo Superior de Investigaciones Científicas (CSIC) I3P predoctoral grant program REF.: I3P-BPD2005.

References

- Álvarez, M., Ríos, A. F., Pérez, F. F., Bryden, H. L., and Rosón, G.: Transports and budgets of total inorganic carbon in the subsolar and temperate North Atlantic, *Global Biogeochem. Cy.*, 17, 1, 1002, doi:10.1029/2002GB001881, 2003.
- Azetsu-Scott, K., Jones, E. P., Yashayaev, I., and Gershey, R. M.: Time series study of CFC concentrations in the Labrador Sea during deep and shallow convection regimes (1991–2000), *J. Geophys. Res.*, 108, C11, 3354, doi:10.1029/2002JC001317, 2003.
- Broecker, W. S., Takahashi, T., Simpson, H. J., and Peng, T. H.: Fate of fossil fuel carbon dioxide and the global carbon budget, *Science*, 206, 409–418, 1979.
- Bryden, H. L., Longworth, H. R., and Cunningham, S. A.: Slowing of the Atlantic meridional overturning circulation at 25°N, *Nature*, 438, 655–657, 2005.
- Corbière A., Metzl, N., Reverdin, G., Brunet, C., and Takahashi, T.: Interannual and decadal variability of the oceanic carbon sink in the North Atlantic subpolar gyre, *Tellus*, doi:10.1111/j.1600-0889.2006.00232.1-11, 2007.
- Curry, R., McCartney, M. S., and Joyce, T. M.: Oceanic transport of subpolar climate signals to mid-depth tropical waters, *Nature*, 391, 575–577, 1998.
- Dickson, R. R., Lazier, J. R. N., Meincke, J., Rhines, P. B., and Swift, J. H.: Long-term coordinated changes in the convective activity of the North Atlantic, *Prog. Oceanogr.*, 38, 241–295, 1996.
- Dickson, B., Yashayaev, I., Meincke, J., Turrell, B., Dye, S., and Holfort, J.: Rapid freshening of the deep North Atlantic Ocean over the past four decades, *Nature*, 416, 832–837, 2002.
- Doney, S. C. and Jenkins, W. J.: The effect of boundary conditions on tracer estimates of thermocline ventilation rates, *J. Mar. Res.*, 46, 947–965, 1988.
- Gruber, N., Sarmiento, J. L., and Stocker, T. F.: An improved method for detecting anthropogenic CO₂ in the oceans, *Global Biogeochem. Cy.*, 10, 809–837, 1996.
- Kieke, D., Rhein, M., Stramma, L., Smethie, N. M., LeBel, D. A., and Zenk, W.: Changes in the CFC inventories and formation rates of Upper Labrador Sea Water, 1997–2001, *J. Phys. Oceanogr.*, 36, 64–86, 2006.
- Kieke, D., Rhein, M., Stramma, L., Smethie, W. M., Bullister, J. L., and LeBel, D. A.: Changes in the pool of Labrador Sea Water in the subpolar North Atlantic, *Geophys. Res. Lett.*, 34, L06605, doi:10.1029/2006GL028959, 2007.
- Lazier, J., Hendry, R., Clarke, R. A., Yashayaev, I., and Rhines, P.: Convection and restratification in the Labrador Sea, 1990–2000, *Deep-Sea Res.*, 49, 1819–1835, 2002.
- Lefèvre, N., Watson, A. J., Olsen, A., Ríos, A. F., Pérez, F. F., and Johannessen, T.: A decrease in the sink for atmospheric CO₂ in the North Atlantic, *Geophys. Res. Lett.*, 31, doi:10.1029/2003GL018957, 2004.
- Lherminier, P., Mercier, H., Gourcuff, C., Alvarez, M., Bacon, S., and Kermabon, C.: Transports across the 2002 Greenland-Portugal Ovide section and comparison with 1997, *J. Geophys. Res.*, 112, C07003, doi:10.1029/2006JC003716, 2007.
- McManus, J. F., Francois, R., Gherhardi, J.-M., Keigwin, L. D., and Brown-Leger, S.: Collapse and rapid resumption of Atlantic meridional circulation to deglacial changes, *Nature*, 428, 834–837, 2004.
- Mikaloff-Fletcher, S. E., Gruber, N., Jacobson, A. R., Doney, S. C., Dutkiewicz, S., Gerber, M., Follows, M., Joos, F., Lindsay, K., Menemenlis, D., Mouchet, A., Müller, S. A., and Sarmiento,

- J. L.: Inverse estimates of anthropogenic CO₂ uptake, transport, and storage by the ocean, *Global Biogeochemical Cy.*, 20, GB2002, doi:10.1029/2005GB002530, 2006.
- Olsson, K. A.: Halogenated tracers and studies of deep and intermediate waters in the Nordic Seas, PhD Thesis, Goteborg University, 1–68, 2001.
- 5 Pickart, R. S., Straneo, F., and Moore, G. W. K.: Is Labrador Sea Water formed in the Irminger Basin?, *Deep Sea Res.*, Part I, 50, 23–52, 2003.
- Sabine, C. L., Feely, R. A., Gruber, N., Key, R. M., Lee, K., Bullister, J. L., Wanninkhof, R., Wong, C. S., Wallace, D. W. R., Tilbrook, B., Millero, F. J., Peng T.–H., Kozyr, A., Ono, T., and Ríos, A. F.: The oceanic sink for anthropogenic CO₂. *Science* 305, 367–371, 2004.
- 10 Sarmiento, J. L. and Le Quéré, C.: Oceanic carbon dioxide uptake in a model of century-scale global warming, *Science*, 274, 1346–1350, 1996.
- Schuster, U. and Watson, A. J.: A variable and decreasing sink for atmospheric CO₂ in the North Atlantic, *J. Geophys. Res.*, 112, C11006, doi:10.1029/2006JC003941, 2007.
- Stramma, L., Kieke, D., Rhein, M., Schott, F., Yashayaev, I., and Koltermann, K. P.: Deep Water changes at the western boundary of the subpolar North Atlantic, 1996–2001, *Deep Sea Res.*, Part I, 51, 1033–1056, 2004.
- 15 Tanhua, T. and Wallace, D. W. R.: Consistency of TTO-NAS inorganic carbon data with modern measurements, *Geophys. Res. Lett.*, 32, L14618, doi:10.1029/2005GL023248, 2005.
- Yashayaev, I. and Dickson, R. R.: Transformation and fate of overflows in the northern North Atlantic, in: “Arctic-Subarctic Ocean Fluxes: defining the role of the Northern Seas in climate”, edited by: Robert, R., Dickson, J., Meincke, P., Rhines., Springer, P.O. Box 17, 3300 AA Dordrecht, The Netherlands, 505–526, 2008.
- 20 Wallace, D. W. R.: Storage and transport of Excess CO₂ in the Oceans: The JGOFS/WOCE Global CO₂ Survey, *Ocean Circulation and Climate*, 489–521, 2001.
- 25 Watson, A. J., Nightingale, P. D., and Cooper, D. J.: Modeling atmosphere-ocean CO₂ transfer, *Philos. Trans. R. Soc., Ser. B*, 348, 125–132, 1995.

1601

Table 1. Summary of cruises showing the analytical precision of the measurements for the main variables used in C_{ant} estimation. NM means “Not Measured” and NA stands for “No Adjustment made”. In any case, units for C_T, A_T and oxygen (O) are in μmol·kg⁻¹.

Cruise	Date	P.I.	Analytical Precision				Adjustment	
			C _T	A _T	pH	O	C _T	A _T
TTO-NAS	07/23–08/14/1981	T. Takahashi	±3.5	±3.7	NM	±1.0	-3.0	-3.6
AR7E	04/8–05/2/1991	H. M. van Aken	±1.3	NM	NM	±0.5	NA	NA
FOUREX	08/7–09/17/1997	S. Bacon	±3.0	±2.0	±0.002	±1.0	NA	NA
OVIDE 02	06/11–07/11/2002	H. Mercier	±3.0	±2.0	±0.002	±0.5	NA	NA
OVIDE 04	06/5–07/6/2004	T. Huck	±3.0	±2.0	±0.002	±0.5	NA	NA
OVIDE 06	05/24–06/26/2006	P. Lherminier	±3.0	±2.0	±0.002	±0.5	NA	NA

1602

Table 2. Temporal evolution from 1981 until 2006 in the five considered water masses of the average values of thickness, salinity, potential temperature, AOU, C_{ant} , percentage of C_{ant}^{sat} and percentage contribution to the specific inventory of C_{ant} in each year.

Year	Thick-ness (m)	Salinity	$\theta(^{\circ}\text{C})$	AOU ($\mu\text{mol}\cdot\text{kg}^{-1}$)	C_{ant} ($\mu\text{mol}\cdot\text{kg}^{-1}$)	% C_{ant}^{sat}	%Inventory
<i>Subsurface layer</i>							
1981	419	34.902±0.001	5.118±0.005	20.4±0.3	29.3±1.5	95±5	22.6±1.1
1991	144	34.981±0.002	5.229±0.007	19.0±0.4	34.6±1.8	92±5	8.0±0.4
1997	414	34.893±0.001	5.134±0.003	21.0±0.1	38.8±0.8	92±2	20.7±0.4
2002	405	34.949±0.001	5.362±0.003	24.6±0.2	42.1±0.8	90±2	22.3±0.4
2004	556	34.967±0.001	5.611±0.002	23.8±0.1	43.5±0.6	89±1	30.3±0.4
2006	552	34.973±0.001	5.587±0.002	23.7±0.1	43.4±0.6	86±1	29.6±0.4
<i>uLSW</i>							
1981	829	34.865±0.001	3.539±0.004	28.1±0.2	25.2±1.2	84±5	38.4±1.8
1991	713	34.889±0.001	3.577±0.004	24.2±0.2	31.3±0.9	86±3	35.8±1.0
1997	506	34.869±0.001	3.520±0.003	35.9±0.1	32.1±0.7	79±2	21.0±0.4
2002	686	34.896±0.001	3.803±0.003	35.0±0.1	33.7±0.6	75±2	30.2±0.5
2004	673	34.888±0.001	3.710±0.003	37.2±0.1	33.2±0.7	71±2	27.9±0.6
2006	646	34.901±0.001	3.822±0.002	34.1±0.1	34.4±0.6	70±2	27.5±0.4
<i>cLSW</i>							
1981	557	34.918±0.002	3.375±0.006	39.2±0.4	18.6±1.7	62±9	19.1±1.8
1991	970	34.878±0.001	3.137±0.004	32.5±0.2	24.6±0.9	68±3	38.1±1.3
1997	983	34.868±0.001	2.989±0.003	30.8±0.1	29.9±0.7	74±2	37.8±0.9
2002	678	34.897±0.001	3.185±0.003	38.8±0.2	27.2±0.7	61±3	24.1±0.6
2004	546	34.902±0.001	3.232±0.004	40.5±0.2	26.8±0.9	58±3	18.3±0.6
2006	529	34.920±0.001	3.355±0.003	40.6±0.2	27.1±0.8	56±3	17.8±0.5
<i>NEADW</i>							
1981	686	34.948±0.001	2.980±0.004	44.3±0.3	14.1±1.2	47±9	17.7±1.6
1991	746	34.940±0.001	2.925±0.003	48.4±0.1	12.9±0.8	36±6	15.4±0.9
1997	754	34.924±0.001	2.813±0.004	44.2±0.2	18.5±1.0	46±5	18.0±0.9
2002	762	34.917±0.001	2.759±0.002	43.7±0.1	20.7±0.7	47±3	20.6±0.7
2004	755	34.916±0.001	2.753±0.003	44.4±0.2	21.7±0.8	47±4	20.5±0.8
2006	787	34.929±0.001	2.850±0.003	43.2±0.1	22.1±0.8	46±3	21.5±0.7
<i>DSOW</i>							
1981	98	34.892±0.002	1.680±0.010	36.6±0.4	12.7±2.5	43±20	2.3±0.4
1991	134	34.897±0.001	1.778±0.005	41.6±0.2	12.7±1.2	36±9	2.7±0.3
1997	94	34.894±0.002	1.720±0.008	38.8±0.4	19.8±2.2	50±11	2.4±0.3
2002	110	34.887±0.001	1.721±0.004	39.4±0.2	18.7±1.3	43±7	2.7±0.2
2004	112	34.869±0.001	1.534±0.004	36.3±0.2	21.1±1.1	47±5	3.0±0.2
2006	132	34.906±0.001	1.866±0.005	37.6±0.2	21.6±1.0	46±4	3.5±0.2

1603

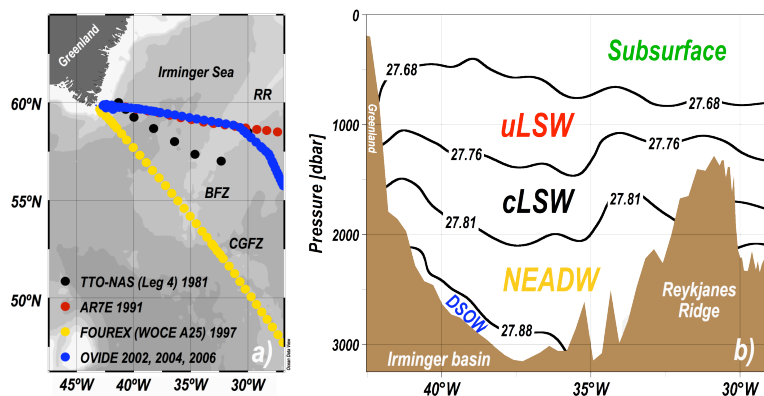


Fig. 1. (a) Map showing the Irminger Sea ends of the North Atlantic cruises used to assess the temporal evolution of the C_{ant} storage. The acronyms stand for: RR=Reykjanes Ridge, BFZ=Bight Fracture Zone and CGFZ=Charlie Gibbs Fracture Zone. (b) Main water masses (cLSW=classical Labrador Seawater; uLSW=upper Labrador Seawater; NEADW=North East Atlantic Deep Water; DSOW=Denmark Strait Overflow Water) present in the Irminger basin and analysed in terms of C_{ant} inventory distributions over time. The density (σ_{θ} in kgm^{-3}) boundaries were established following Kieke et al. (2007) and Yashayaev et al. (2007).

1604

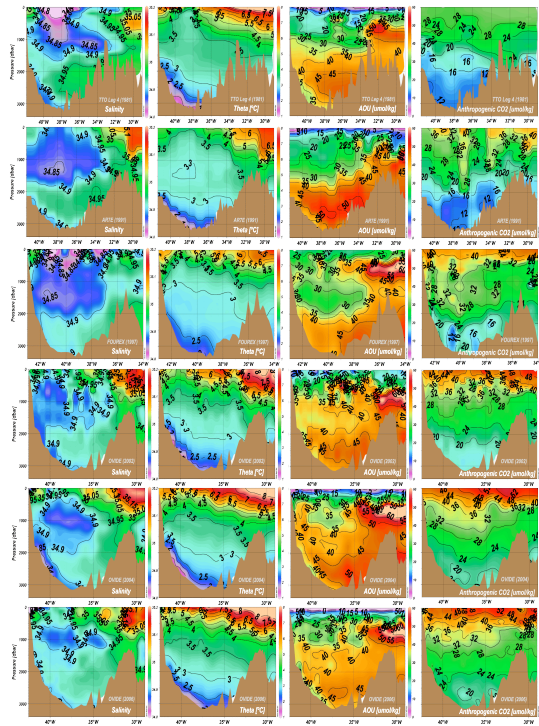


Fig. 2. Vertical profiles of Salinity, potential temperature (θ , in Celsius degrees), AOU ($\mu\text{mol}\cdot\text{kg}^{-1}$) and C_{ant} ($\mu\text{mol}\cdot\text{kg}^{-1}$) for the six cruises shown in Fig. 1a. The colour scale in each of the variables is the same for all years to facilitate comparison. The dataset shown in these contour plots is the one used to compute C_{ant} storages and make further analysis.

1605

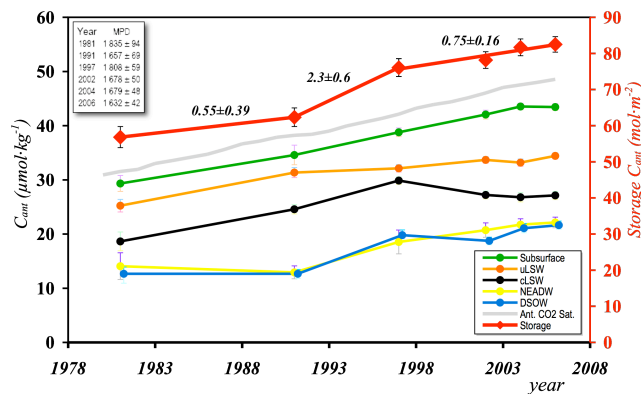


Fig. 3. Temporal evolution (1981–2006) of the average C_{ant} ($\mu\text{mol}\cdot\text{kg}^{-1}$) stored in the subsurface layer (green line), uLSW (orange line), cLSW (black line), NEADW (yellow line) and DSW (blue line). The continuous grey line shows the 100% C_{ant} saturation of water masses in equilibrium with the atmosphere over time, following the atmospheric CO_2 increase. The evolution of the specific inventory (in $\text{mol}\cdot\text{C}\cdot\text{m}^{-2}$) of C_{ant} in the Irminger basin is given by the thick red line, and its values can be read on the right-hand y-axis. The numbers above this line stand for the C_{ant} storage increase rates (in $\text{mol}\cdot\text{C}\cdot\text{m}^{-2}\cdot\text{yr}^{-1}$) for the time periods of 1981–1991, 1991–1997 and 1997–2006. The table on the top-left corner shows the temporal variability of the mean penetration depth (MPD, in meters).

1606